Preliminary photoacoustic imaging of the human radial artery for simultaneous assessment of red blood cell aggregation and oxygen saturation *in vivo*

Tae-Hoon Bok Eno Hysi Michael C. Kolios

Department of Physics, Ryerson University,
Institute for Biomedical Engineering, Science and Technology (iBEST), a partnership between Ryerson University and St. Michael's Hospital,
Keenan Research Centre for Biomedical Science of St. Michael's Hospital
Toronto, Canada

tbok@ryerson.ca eno.hysi@ryerson.ca mkolios@ryerson.ca

Abstract*— Our group has previously demonstrated that lower shear rate in the pulsatile blood flow yields greater red blood cell (RBC) aggregation which in turn results in a higher oxygen saturation (sO_2) level and a higher photoacoustic (PA) signal. Higher shear rates led to disaggregation thereby decreasing the PA signal amplitude and the sO_2. These results suggest that the interrelationship between the sO_2 and RBC aggregation may provide a new biomarker in the diagnosis of diseases that alter blood rheological properties. In this paper, we present a pilot study where high-frequency photoacoustic imaging (PAI) is used for the simultaneous assessment of RBC aggregation and sO_2 *in vivo* in the human radial artery (RA). The ultrasound (US) and PA images in the RA were acquired using a US/PA imaging system equipped with a 21 MHz linear-array probe (Vevo LAZR; LZ250, FUJIFILM VisualSonics, Canada), varying the wavelength of optical illumination (700, 750, 800, 850 and 900 nm). The blood flow velocity at the RA was assessed by pulsed wave Doppler in the same device. The PA signals inside the RA were observed at all wavelengths. The PA power increased with the illumination wavelength. At each wavelength, the PA power varied as function of time. The phase of variation in PA signals was inversely proportional to that in systolic blood flow velocity. The sO_2 is proportional to the cell surface area exposed to the surrounding media, and RBC aggregation decreases the exposed area of the aggregate. As such, the sO_2 was higher for aggregated cells (diastolic state) than single cells (systolic state). This PAI study of RA RBC aggregation and sO_2 *in vivo* is the first attempt to study the hemodynamics and physiological function of RBC, which can be used as a potential tool for the diagnosis of blood flow conditions in the RA.

Keywords—red blood cell aggregation, oxygen saturation, photoacoustic imaging, radial artery

I. INTRODUCTION

The main physiological function of red blood cell (RBC) is the delivery of oxygen to tissues and the oxygen delivery is controlled by the oxygen saturation (sO_2) [1]. In addition, RBCs tend to aggregate when exposed to very low shear rate, e.g. RBC aggregation was measured by 30 MHz of ultrasonic transducer for the shear rate less than 80 s^{-1} [2]. The aforementioned physiological function and hemodydnamic structure were investigated in terms of their interrelationship [3], exploring how the diffusion of oxygen from RBCs is inhibited by RBC aggregation. This phenomenon was demonstrated by photoacoustic imaging (PAI) of the pulsatile blood flow *in-vitro*, conducted by our group [4].

The radial artery is easy accessible and can be a surrogate to measure the central blood pressure [5], which is related to the blood flow velocity and the pulsation due to the vessel wall stiffness. In the present paper, we investigate the preliminary clinical application of the PAI of the pulsatile blood flow in the human radial artery, based on our previous study on RBC aggregation and sO_2 measured by PAI [4]. The present study is, to our knowledge, the first report to measure RBC aggregation and sO_2 by photoacoustics in human body.

II. MATERIALAS AND METHODS

A. US/PA imgaing system

A commercialized linear-array probe based PAI system [6], [4] (Vevo LAZR; LZ250, FUJIFILM Visualsonics, Toronto, ON, Canada) was employed in order to conduct this study. Tunable illumination wavelengths from 680 nm to 970 nm were generated by a Nd:YAG laser combined with an optical parameter oscillator. 700, 750 800, 850 and 900 nm were chosen for our experiments in order to interpret the PA amplitude as a function of the λ around an isosbestic point, 800 nm. Each laser pulse had a duration of around 10 ns, and a pulse repetition rate of 20 Hz. Two rectangular (0.88 mm in the elevation direction and 25.35 mm in the longitudinal direction) optical fiber bundles were parallel separated by 5.75 mm from the inner edge of the fibers in the elevation direction. The laser beam from each fiber bundle had a divergence angle of 24º in water and an incident angle of ±30º, converging on the range of 3.19 to 11.56 mm in the axial direction. The incident laser fluence was less than 5 mJ/cm^2, below the safety limit by the American National Standards for these wavelengths. PA signals were detected by a 256-element linear-array transducer with a central frequency of 21 MHz, a bandwidth between 13

978-1-5386-3383-0/17/$31.00 ©2017 IEEE

and 24 MHz, and an aperture length of 23.04 mm. The data acquisition system contained only 64 channels, which resulted in the full field of view consisting of four quadrants in the longitudinal direction [7], as shown in Fig. 1.

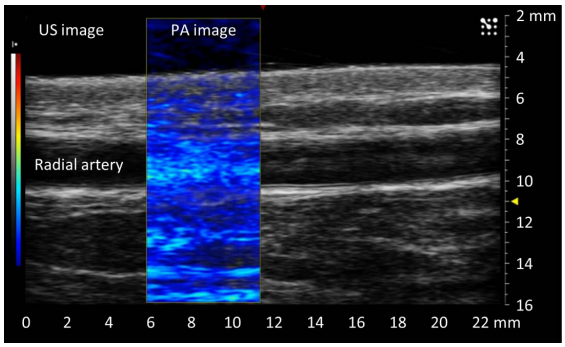

Fig. 1. Example of ultrasound (US) and photoacoustic (PA) images from the human radial artery. The PA image was acquired from the second quadrant in order to maximize the frame rate and avoid the edge effect of the finite elements of transducer.

B. *Measurement protocol*

The present human participant experiment was approved by the Research Ethic Board of Ryerson University (REB 2017-040). Consent forms were signed by all participants after being briefed on the purpose of the study, the experimental process, and the possible risks involved. As a measurement protocol, the participants were asked to do the following:

1) do not drink alcohol for 8 to 10 hours, and do not smoke for one hour before the study begins.
2) provide demographic data (age, gender), and be measured for height and weight. These data were recorded in a spreadsheet (confidentially coded). BMI was calculated using height and weight data.
3) sit down on a chair, and rest their left arm in a water bath on a table.
4) allow the degassed warm (36 ºC) water to be filled in the bath.
5) allow the tester to gently immerse the photoacoustic probe above their wrist.
6) allow the tester to find the radial artery using the Doppler mode (the laser was off)
7) allow the tester to record the blood flow velocity using the Doppler mode.
8) wear laser safety goggles for the duration of the photoacoustic measurements.
9) allow the tester to record images as both visible and invisible light waves were transmitted into the wrist with a laser fluence < 5 mJ/cm^2 (safety limit of the American National Standards Institute)
   → five wavelengths (700, 750, 800, 850, 900 nm)

C. *Post-processing*

In the US B-mode image, the 65th to 128th channel were selected as shown in Fig. 1(a). From the envelop of a US backscatter RF signal, the location of two maximum peaks (which corresponded to the top and bottom walls) were extracted, and the vessel diameter was estimated. Thereafter, the location of 10% margin from both walls were estimated, and were considered as the top and bottom boundaries for the region of interest (ROI) as shown in Fig. 2(b). This procedure was performed for 64 signals at each frame. The ROI of the US signals was applied to extracting the ROI of PA signals, as show in Figs. 2(c) and 2(d). The root mean square (RMS) of the PA signal in the ROI was computed for each channel (64 channel in total), and 64 RMS were averaged and taken by log scale in equation (1). This process was repeated for all frames at all λ.

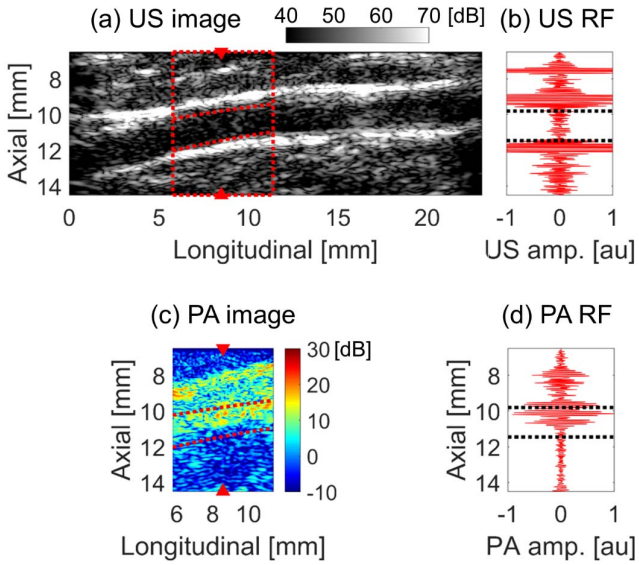

Fig. 2. (a) The reconstructed US image and the acquisition area of 64 PA channels (red-dotted box). The red-dotted lines represent the top and bottom boundaries for the region of interest. (b) The US RF signal at the location of the 32nd channel of PA signals. The black-dotted line represent the top and bottom boundaries. The reconstructed PA image (c) and the PA RF signal at the location of the 32nd channel of PA signals (d). The top and bottom boundaries are consistent with those from the US image.

$$\text{PA power} = 20\log_{10}\left(\sqrt{\frac{1}{n}\sum_{z=z_1}^{z_n} p(z)^2}\right) \text{ [dB]} \qquad (1)$$

In equation 1, n is the sample number of the ROI, z is the axial depth from z_1 (top boundary) to z_n (bottom boundary), $p(z)$ is the PA amplitude at a depth z.

III. Results and Discussion

The blood flow velocity cyclically varied with 18 cm/s of the peak systolic velocity and 0.5 cm/s of the end diastolic velocity while the heartbeat rate was 77 bpm as shown in Fig. 3 (blue line). The vessel diameter expanded up to 2.45 mm and contracted to 2.3 mm at the peak systole and end diastole, respectively, as shown in Fig. 3 (red line). The pulsatile flow generates the cyclic variation in the shear stress at the blood vessel wall, and the vessel expands and contracts during the systole and diastole in the artery [8]. Given the relationship between the pulsatile flow and the vessel

978-1-5386-3383-0/17/$31.00 ©2017 IEEE

expansion/contraction, the vessel diameter was estimated by post-processing and could be manually synchronized.

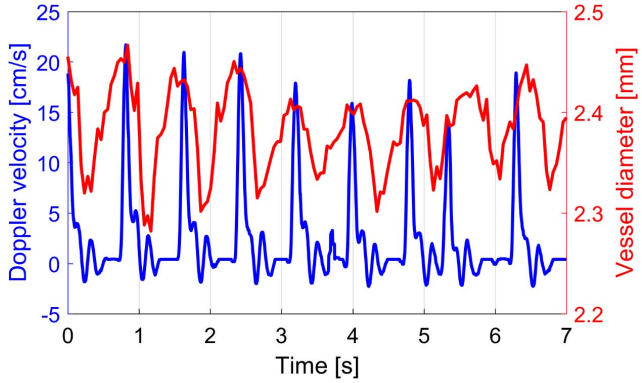

Fig. 3. The Doppler velocity (blue) and vessel diameter (red) as a function of time. The Doppler velocity cyclically varies due to the pulsatile flow induced by the heartbeat, so that the vessel diameter also cyclically varies.

The PA power cyclically varied for all λ as shown in Fig. 4a. The cyclic variation in the PA power was consistent with the *in-vitro* measurement conducted by our group [4]. This phenomenon under the *in-vitro* condition was thought to be due to the cyclic variation in RBC aggregation and disaggregation affecting the effective absorber size [9]. In the same way, the cyclic variation in the PA power under the *in-vivo* condition could be interpreted to be the same as the results under the *in-vitro* condition. The average of the PA power and the corresponding standard deviation increased with the λ as shown in Figs. 4b and 4c.

The increase in the PA power with the λ is due to the increase of the optical absorption coefficient (μ_a) of the RBC as a function of λ, according to the theoretical and *in-vitro* experimental results [10], [11]. The increase of the SD representing the magnitude of cyclic variation in the PA power could be interpreted using the molar extinction coefficients of oxyhemoglobin (ε_{HbO}) and deoxyhemoglobin (ε_{Hb}) as a function of λ. The ε_{HbO} and ε_{Hb} increase with the λ from 700 nm to 900 nm (an isosbestic point at 800 nm) [12]. For the λ > 800 nm, the increase of ε_{HbO} is steeper than that of ε_{Hb}. This suggests that the μ_a of RBC for higher sO_2 is higher than that for lower sO_2, and the μ_a difference between higher and lower sO_2 increases with the λ. For the λ < 800 nm, the decrease of ε_{HbO} is steeper than that of ε_{Hb}, resulting in the μ_a of RBCs for higher sO_2 is lower than that for lower sO_2. This results in the μ_a difference between higher and lower sO_2 increasing with the shorter optical wavelengths.

The PA power is theoretically proportional to the size and the μ_a of optical absorber [13], and the size is independent of the μ_a. However, it was found that the size and μ_a of the absorber under the pulsatile blood flow were related to each other [4], [3]. RBC aggregation increases the absorber size regardless of the λ, and simultaneously increases the sO_2 for λ > 800 nm, thus resulting in increase of the μ_a. In this case, the PA power is affected by both the increased size and increased μ_a, so that the magnitude of the cyclic variation in the PA power is relatively larger for λ > 800 nm (Figs. 4a and c). On the other hand, RBC aggregation decreases the sO_2 for the λ shorter than 800 nm, resulting in a decrease of the μ_a. In this case, even if the PA power is affected by the increased aggregate size, it is also affected by a decreased RBC μ_a. Therefore, the magnitude of the cyclic variation in the PA power is relatively smaller for the λ shorter than 800 nm (Fig. 4a).

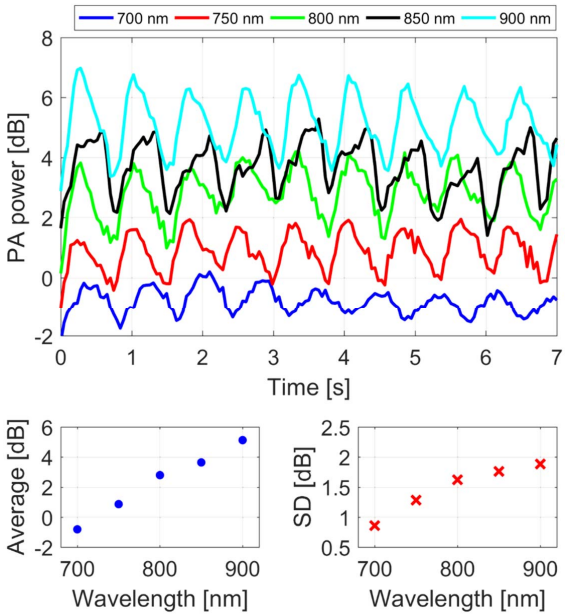

Fig. 4. The PA power as a function of time (a), the average of PA power (b) and the corresponding standard deviation, SD (c), at each wavelength.

The estimated sO_2 cyclically varied from 76% to 88%, and the mean sO2 was 82%, as show in Fig. 5. The mean sO_2 was relatively lower than the normal sO_2 in the artery which is between 96% and 99% [1]. This can be due to the fact that no fluence correction was applied to the estimation of the sO_2. Nevertheless, the cyclical variation of the sO_2 is significant despite the fact that the absolute value is not known. This result could be clinically meaningful since the physiological function of RBC can be potentially monitored in real-time by the PAI while examining the *in-vivo* interrelationship between the hemodynamic phenomena and the oxygen transport.

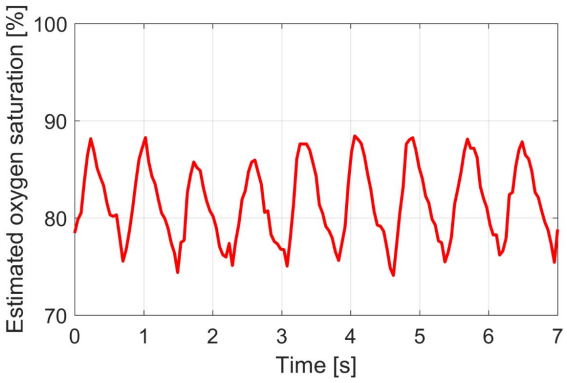

Fig. 5. The oxygen saturation, estimated by the two-wavelength method, as a function of time.

978-1-5386-3383-0/17/$31.00 ©2017 IEEE

IV. Conclusion

In this paper, the human radial artery was imaged by photoacoustics in the range of optical wavelength of 700 nm to 900 nm and an ultrasonic frequency of 21 MHz. The PA power increased with the λ, and cyclically varied with a period equal to the heartbeat rate, at each wavelength. The pulsatile flow in the artery induced cyclic variation in RBC aggregation and disaggregation resulting in cyclic variation in the PA power. In addition, estimates of the sO_2 also cyclically varied with a period of the heartbeat rate. The sO_2 increased and decreased during RBC aggregation and disaggregation, respectively. This study is the first report to investigate RBC aggregation and sO_2 by PAI in the radial artery while examining hemodynamic parameters of blood flow.

Acknowledgment

This work was funded by Natural Sciences and Engineering Research Council of Canada / Canadian Institutes of Health Research - Collaborative Health Research Projects grant # 462315-2014. Funding to purchase the equipment was provided by the Canada Foundation for Innovation, the Ontario Ministry of Research and Innovation, and Ryerson University. E. Hysi is supported by a Vanier Canada Graduate Scholarship.

References

[1] T. R. Des Jardins, *Cardiopulmonary Anatomy and Physiology: Essentials for Respiratory Care*, 4th ed. New York: Delmar, 2002.

[2] M. S. van der Heiden, M. G. M. de Kroon, N. Bom, and C. Borst, "Ultrasound backscatter at 30 MHz from human blood: Influence of rouleau size affected by blood modification and shear rate," *Ultrasound Med. Biol.*, vol. 21, no. 6, pp. 817–826, 1995.

[3] N. Tateishi, Y. Suzuki, I. Cicha, and N. Maeda, "O2 release from erythrocytes flowing in a narrow O2-permeable tube: effects of erythrocyte aggregation," *Am. J. Physiol. - Hear. Circ. Physiol.*, vol. 281, no. 1, pp. H448–H456, 2001.

[4] T.-H. Bok, E. Hysi, and M. C. Kolios, "Simultaneous assessment of red blood cell aggregation and oxygen saturation under pulsatile flow using high-frequency photoacoustics," *Biomed. Opt. Express*, vol. 7, no. 7, pp. 2769–2780, 2016.

[5] K. Takazawa, H. Kobayashi, N. Shindo, N. Tanaka, and A. Yamashina, "Relationship between radial and central arterial pulse wave and evaluation of central aortic pressure using the radial arterial pulse wave.," *Hypertens. Res.*, vol. 30, no. 3, pp. 219–228, 2007.

[6] A. Needles, A. Heinmiller, J. Sun, C. Theodoropoulos, D. Bates, D. Hirson, M. Yin, and F. Foster, "Development and initial application of a fully integrated photoacoustic micro-ultrasound system," *IEEE Trans. Ultrason. Ferroelectr. Freq. Control*, vol. 60, no. 5, pp. 888–897, 2013.

[7] P. Ephrat, A. Needles, C. Bilan, A. Trujillo, C. Theodoropoulos, D. Hirson, and S. Foster, "White paper: Imaging of murine tumors using the Vevo® LAZR photoacoustic imaging system," 2010.

[8] M. Eriksen, "Effect of pulsatile arterial diameter variations on blood flow estimated by Doppler ultrasound.," *Med. Biol. Eng. Comput.*, vol. 30, no. 1, pp. 46–50, 1992.

[9] E. Hysi, R. K. Saha, and M. C. Kolios, "Photoacoustic ultrasound spectroscopy for assessing red blood cell aggregation and oxygenation," *J. Biomed. Opt.*, vol. 17, no. 12, p. 125006, 2012.

[10] T.-H. Bok, E. Hysi, and M. C. Kolios, "Effect of optical wavelength on photoacoustic investigations of pulsatile blood flow," in *Proceedings of SPIE*, 2016, vol. 9708, p. 97081M.

[11] T.-H. Bok, E. Hysi, and M. C. Kolios, "Quantitative photoacoustic assessment of red blood cell aggregation under pulsatile blood flow: experimental and theoretical approaches," in *Proceedings of SPIE*, 2017, p. 100645F.

[12] S. Prahl, "Optical Absorption of Hemoglobin," 2015. [Online]. Available: http://omlc.org/spectra/hemoglobin/.

[13] G. J. Diebold, "Photoacoustic monopole radiation: waves from objects with symmetry in one, two and three dimensions," in *Photoacoustic Imaging and Spectroscopy*, L. V. Wang, Ed. Boca Raton, FL: CRC Press, 2009, pp. 3–17.